

Search for Threshold Behavior in DIII-D Electron Heat Transport

T.C. Luce, J.C. DeBoo, N. Howard,¹ C. Liu, and C.C. Petty

General Atomics, P.O. Box 85608, San Diego, California 92186-5608, USA
 University of Illinois, Champaign, Illinois, USA

I. Introduction

Theoretical models of heat transport in tokamaks often predict a significant increase in transport when a threshold is reached. It is difficult to test for thresholds using power balance analysis or the temperature profiles directly [1]. However, modulation of the electron temperature by electron cyclotron heating (ECH) may be a means to test for thresholds, since the incremental heat flux is probed more directly. Experiments in AUG [2] and DIII-D [3] designed to vary the equilibrium temperature gradient have been carried out under similar conditions. ECH is applied at two radii in the plasma. The total power is fixed, so the equilibrium temperature outside the outer heating point is constant. The power mixture is varied in order to change the equilibrium temperature gradient in the region between the two heating points. Plasmas with L-mode edge and early heating are used to avoid the effects of ELMs and sawteeth on the modulation analysis. No other auxiliary heating is used during the time of the ECH. The quantity $R|\nabla T|/T$ varies from 6.2–10.3 at the midpoint between the two heating positions. This variation is mostly in the gradient, as the equilibrium temperature varies less than $\pm 10\%$.

II. Framework for Analysis of Modulation Data

In order to interpret the modulation data, the energy conservation equation in the form

$$\frac{3}{2}n \frac{\partial T}{\partial t} + \frac{1}{H\rho} \frac{\partial}{\partial \rho} (H\rho q) = Q \quad , \quad q = -n\chi(\rho, T, \nabla T) \nabla T + nU(\rho, T) T + \xi(\rho) \quad (1)$$

is used. The first term in the heat flux q is diffusive, the second is convective, and the third allows for the possibility of heat flux independent of temperature. The quantity H is a geometric factor. A small periodic perturbation around an equilibrium is assumed:

$$T = T_0 + T_1 e^{i\omega t}, \quad \partial T_0 / \partial t = 0 \quad , \quad |T_1| / T_0 \ll 1 \quad . \quad (2)$$

Linearizing Eq. (1) with the assumptions of Eq. (2) gives:

$$-D \frac{d^2 T_1}{d\rho^2} + V \frac{dT_1}{d\rho} + \frac{1}{\tau} \left(1 + i \frac{3}{2} \omega \tau \right) T_1 = S_1 \quad , \quad (3)$$

where

$$D \equiv \chi_0 + \frac{\partial \chi}{\partial (\nabla T)} \frac{dT_0}{d\rho} \quad , \quad (4)$$

$$V \equiv -\frac{1}{n} \frac{dn}{d\rho} \chi - \frac{\partial \chi}{\partial \rho} - \frac{1}{H\rho} \frac{d(H\rho)}{d\rho} \chi + U + \frac{\partial U}{\partial T} T_0$$

$$- \left[\frac{1}{n} \frac{dn}{d\rho} \frac{\partial \chi}{\partial (\nabla T)} + \frac{\partial^2 \chi}{\partial \rho \partial (\nabla T)} + \frac{\partial \chi}{\partial T} + \frac{1}{H\rho} \frac{d(H\rho)}{d\rho} \frac{\partial \chi}{\partial (\nabla T)} \right] \frac{dT_0}{d\rho} - \frac{\partial \chi}{\partial (\nabla T)} \frac{d^2 T_0}{d\rho^2} \quad , \quad (5)$$

$$\begin{aligned}
\frac{1}{\tau} \equiv & -\frac{\partial \chi}{\partial T} \frac{dT_0}{d\rho^2} + \left[\frac{\partial U}{\partial T} - \frac{1}{n} \frac{dn}{d\rho} \frac{\partial \chi}{\partial T} - \frac{\partial^2 \chi}{\partial \rho \partial T} - \frac{1}{H\rho} \frac{d(H\rho)}{d\rho} \frac{\partial \chi}{\partial T} \right] \frac{dT_0}{d\rho} \\
& + \left[\frac{1}{n} \frac{dn}{d\rho} \frac{\partial U}{\partial T} + \frac{\partial^2 U}{\partial \rho \partial T} + \frac{1}{H\rho} \frac{\partial \chi}{\partial T} \frac{d(H\rho)}{d\rho} \frac{\partial U}{\partial T} \right] T + \frac{1}{n} \frac{dn}{d\rho} U + \frac{\partial U}{\partial \rho} \\
& + \frac{1}{H\rho} \frac{d(H\rho)}{d\rho} U + \frac{3}{2} \frac{Q_{OH}}{nT_0} + \frac{Q_{ie}}{2nT_0} \left(\frac{T_0 - 3T_i}{T_0 - T_i} \right), \quad (6)
\end{aligned}$$

and S_1 is the modulated power source. The quantities D , V , and τ are, respectively, an effective diffusivity, convective velocity, and damping.

To gain insight into how the evolution of the heat pulse relates to the effective transport coefficients of Eq. (3), it is helpful to examine the analytic solutions to Eq. (3) in the simplest case — infinite slab, constant D , V , $1/\tau$, and a point source of heat [4]. The solutions are of the form $T_1 \propto e^{k\rho}$, where

$$k \equiv \frac{V}{2D} \pm \left(\frac{3\omega}{2D} \right)^{1/2} (1 + \alpha^2)^{1/4} e^{i(1/2) \tan^{-1}(1/\alpha)}, \quad \alpha \equiv \left(\frac{V^2}{4\omega D} + \frac{1}{\omega\tau} \right) \frac{2}{3}. \quad (7)$$

If $V = 1/\tau = 0$, then $k = \pm(1+i) (3\omega/4D)^{1/2}$. This means, for the purely diffusive case (with the above approximations), the amplitude falls like $\exp[-(3\omega/4D)^{1/2}\rho]$, and the phase increases like $(3\omega/4D)^{1/2}\rho$ away from the source. In this case, the effective diffusivity D can be easily determined from either the amplitude or the phase change with radius:

$$D_{ph} \equiv \left(\frac{3\omega}{4} \right) \left(\frac{d\phi}{dx} \right)^{-2}, \quad D_{amp} \equiv \left(\frac{3\omega}{4} \right) \left(\frac{1}{T_i} \frac{dT_i}{dx} \right)^{-2}. \quad (8)$$

To see how convection and damping affect the evolution of the heat pulse, D_{ph} and D_{amp} can be evaluated for the solution in Eq. (7):

$$D_{ph} \equiv D \left[\alpha + (1 + \alpha^2)^{1/2} \right] \quad (9)$$

$$D_{amp} = D / \left\{ \frac{V^2}{3\omega D} \pm 2 \left(\frac{V^2}{3\omega D} \right)^{1/2} \left[\alpha + (1 + \alpha^2)^{1/2} \right]^{1/2} + \alpha + (1 + \alpha^2)^{1/2} \right\}. \quad (10)$$

These are plotted in Fig. 1 for damping only and convection only. In both cases, the simple estimates of D can be significantly modified. In the case of damping only, the quantity $D_{mix} \equiv (D_{ph} D_{amp})^{1/2} = D$, allowing a way to determine the diffusivity in the presence of damping. When there is an effective convection term, $D_{mix} \neq D$. The direction of the heat pulse relative to the direction of convection affects only D_{amp} . Note that D_{amp}/D is quite large for an effective convection term.

III. Experimental Analysis

Analysis of the DIII-D [3] experiments proceeded by two steps. First, the evolution of the heat pulse was evaluated by D_{mix} at the highest frequency allowed by the data (either fundamental or third harmonic). Then both this estimate for D and the power balance

estimate of χ were plotted against $1/L_T \equiv |\nabla T|/T$. Similar analysis was performed on the AUG data. The enhancement in D_{mix} above χ_{pb} was taken as evidence of an increase in diffusivity with $1/L_T$. In the AUG case, a model of the form:

$$\chi = \chi_0 + \lambda q(\rho) T^{3/2} \left(\frac{-RV\Gamma}{T} - \kappa \right) H \left(\frac{-RV\Gamma}{T} - \kappa \right), \quad (11)$$

was used to interpret the data trends in terms of a critical gradient. All of the data (by this interpretation) lay above the threshold, so the lowest value of R/L_T set an upper limit on the threshold κ . There are two assumptions implicit in this approach. First, it is assumed that $V^2/\omega D$ and $1/\omega\tau$ are sufficiently small that D_{mix} gives D accurately. Second, it is assumed that the V and $1/\tau$ for the model [Eq. (11)] are ignorable at the measurement ω . These assumptions will now be examined in the DIII-D case.

One consistency check that D_{mix} is a good estimate of D is to examine the frequency dependence of D_{ph} . The phase estimate is used because it is independent of the sign of V and the Fourier transform gives a much more reliable estimate of the phase than the amplitude. Table I shows the fundamental and third harmonic estimates D_{ph} for several different mixtures of heating. In all cases, $D_{\text{ph}}(f_{\text{mod}}) < D_{\text{ph}}(3f_{\text{mod}})$, indicating $\alpha < 0$. Since $V^2/\omega D > 0$, this implies $\tau < 0$ or inverse damping. From Eq. (6), it is clear that $\tau < 0$ does not require $U \neq 0$ or $T_i > T_e$. The table also shows that $D_{\text{amp}}(f_{\text{mod}}) > D_{\text{amp}}(3f_{\text{mod}})$ except on the cases with the strongest heating at the inner radius. An example that clearly illustrates the effect of inverse damping (118474) is shown in Fig. 2. The amplitude of the heat pulse at the modulation frequency almost remains constant as the pulse travels in. This cannot be due to a broadened source since the phase clearly shows the pulse appearing at the intended location first, then moving away in both directions. The observation of $\tau < 0$ is consistent with the heat pinch in strong off-axis ECH cases inferred from power balance [5,6] and from modulation [4]. The conclusion is that D_{mix} is likely not a good estimator of D in these cases.

The assumption that the V and $1/\tau$ terms arising from Eq. (11) are negligible seems to be questionable. Figure 3 shows D , V , and $1/\tau$ for the same discharge from which the data in Fig. 2 are taken. Also shown are the dimensionless quantities $\omega D/V^2$

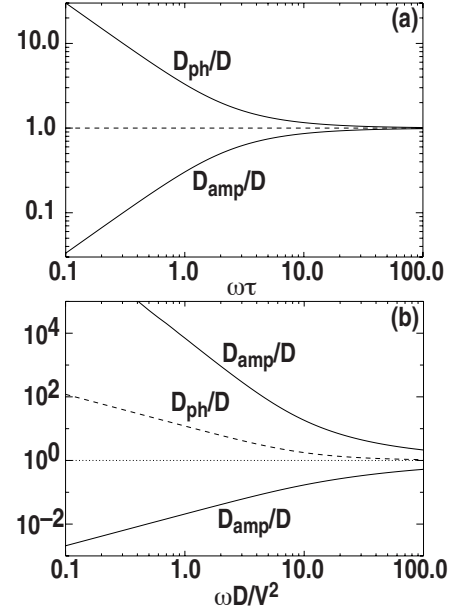


Fig. 1. Slab estimates of diffusivity for the case of (a) diffusion plus damping and (b) diffusion plus convection. The upper curve in (b) is for the case of the heat pulse moving in the direction of the convection.

Table I. Modulation data from DIII-D. All cases follow an inward-moving pulse except 118488.

Shot	Gyro Inner/Outer	Harmonic	D_{amp} (m^2/s)	D_{ph} (m^2/s)	Min R/L_T
118479	0/3.5	1	17.5	2.5	5.6
		3	5.6	9.0	5.9
118476	1/2.5	1	30.5	4.8	4.5
		3	13.1	11.5	7.9
118474	2/1.5	1	630.0	4.5	3.3
		3	6.0	31.9	8.2
118490	3/0.5	1	10.7	7.8	9.6
		3	10.8	11.5	11.4
118488	2.5/1	1	4.3	9.6	—
		3	6.0	37.3	—

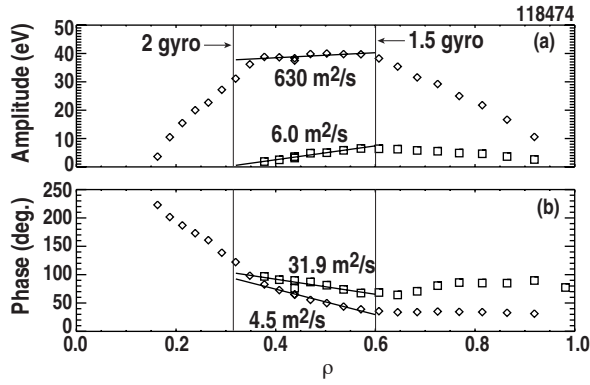


Fig. 2. (a) Amplitude and (b) phase of the heat pulse vs. normalized radius for the fundamental (diamonds) and third harmonic (squares) frequency in the case with two gyrotrons heating at $\rho=0.32$ and one continuous and one modulated gyrotron heating at $\rho=0.6$. The lines show the linear fits used to determine D_{amp} and D_{ph} .

and $\omega\tau$ from Fig. 1. There are regions of strong inverse damping and inward convection, but in the region where the data would require these, the model predicts strong outward convection and damping. The magnitude of these indicate they cannot be neglected in the application of the model.

Simulations of Eq. (4) with D , V , and $1/\tau$ determined from Eq. (11) show that the signature of a critical gradient for heat pulses traveling inward (above threshold to below threshold) would be a rapid drop in amplitude and rise in phase lag. This is very difficult to distinguish from the signal reaching the detection limit. Table I lists the minimum R/L_T at which the pulse remains detectable in the present DIII-D experiments. This serves as an upper limit to the threshold κ . A complementary technique developed on FT-U [7] does not show any evidence of threshold behavior at even smaller values of R/L_T [3].

The DIII-D modulation data show no direct evidence of a threshold above which electron heat transport increases strongly. The upper limits set on such a threshold by the data indicate that the threshold, if it exists, would always be exceeded over most of the plasma radius in auxiliary heated discharges. Furthermore, both the modulation and power balance data are clearly consistent with the existence of a heat pinch. A simulation code has been developed that can treat models like Eq. (11) self-consistently for comparison to modulation data. We will use this to determine the forms of D , V , and $1/\tau$ required to match the amplitude and phase data at multiple frequencies.

Work supported by the U.S. Department of Energy under DE-FC02-04ER54698.

- [1] J.D. Callen, *et al.*, Nucl. Fusion **27**, 1857 (1987).
- [2] F. Ryter, *et al.*, Nucl. Fusion **43**, 1396 (2003).
- [3] J.C. DeBoo, *et al.*, Nucl. Fusion **45**, 494 (2005).
- [4] T.C. Luce, *et al.*, in *Local Transport Studies in Fusion Plasmas*, Editrice Compositori, Bologna, ed. J.D. Callen, G. Gorini, E. Sindoni, 1993, p. 155.
- [5] T.C. Luce, C.C. Petty, J.C.M. deHaas, Phys. Rev. Lett **68**, 552 (1992).
- [6] C.C. Petty, T.C. Luce, Nucl. Fusion **34**, 121 (1994).
- [7] S. Cirant, *et al.*, in Proc. 19th Fusion Energy Conf. Lyon, France (2002), EX/C4-2Rb.

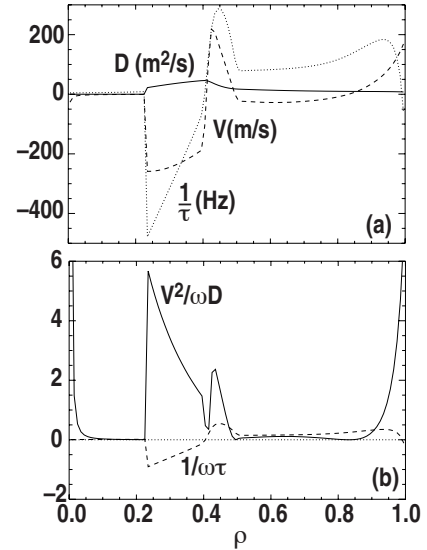


Fig. 3. (a) Evaluation of D , V , $1/\tau$, for the critical gradient model [Eq. (13)] vs normalized radius. The co-efficients used are the same as for AUG [2]. The kinetic profiles are those measured in the same plasma shown in Fig. 2. The reciprocal of the dimensionless parameters from the x-axes on Fig. 1 are shown in (b).